Modeling and Control of a V2G Charging Station Based on the Synchronverter Technology

Dongqi Liu, Qing-Chang Zhong, *Fellow, IEEE,* Yaonan Wang, and Guorong Liu

***Abstract*—In this paper, an idea of modeling and control of a V2G charging station (CS) for electric vehicles (EVs) by using synchronverter technology is proposed. Firstly, the architecture of the CS is introduced, which is composed of several CS units connected in parallel and using synchronverters, which are inverters that mimic synchronous machines, as the AC/DC interfaces between each CS units and the grid. Then, a T-S fuzzy controller is designed to decide the reference real power of the synchronverter by considering the grid frequency, which is estimated by the synchronverter itself, and the energy demand of EVs inside each CS unit. Due to the inner frequency- and voltage-drooping mechanisms of the synchronverter, the input&ouput real and reactive power of the CS will be automatically adjusted on the basis of the reference value according to the degree of deviation from the nominal value of the grid frequency and voltage. To ensure the safety of this operation, an adaptive frequency droop coefficient mechanism is designed to adapt the change of the total energy storage of a CS unit by changing the slope of the P-f control characteristic of the synchronverter. By using the proposed method, a CS can be integrated into the power grid and behave in the same way as large synchronous generator&motor do, thus the CS and the power grid can be held as a whole based on the well-known synchronous mechanism. It is able to provide the grid damping and inertia, which would help the operation of the grid be smoother, and is able to not only realizing bi-directional charging for electric vehicles but also providing high-quality frequency and voltage regulation services for the grid. The performance of the CS with the proposed control strategy is investigated with EVs of different battery states, different user's sets and under different grid status. Simulation results demonstrate that the proposed strategy can not only effectively perform controlled charging/discharging of each single electric vehicle inside the CS, but can improve the performance of the electricity grid in terms of efficiency, stability, and reliability as well.**

***Index Terms*—Electric vehicle(EV), Synchronverter, Vehicle-to-Grid(V2G), Smart Grid, Virtual Synchronous Machines(VSM).**

I. INTRODUCTION

Manuscript received xx xx, 20xx; revised xx xx, 20xx. The work of D.Liu was supported by the China Scholarship Council under Grant 201506130036, with the award of a scholarship (2015-2016).

D. Liu is with the School of Electrical and Information Engineering, Changsha University of Science&Technology, Changsha, 410114 China and the College of Electrical and Information Engineering, Hunan University, Changsha, 410082 China. He was with the Department of Electrical and Computer Engineering, Illinois Institute of Technology, Chicago, IL 60616 USA (e-mail: liu.dongqi@hotmail.com).

Q. Zhong is with the Electrical and Computer Engineering Department, Illinois Institute of Technology, Chicago, IL 60616 USA (e-mail: zhongqc@ieee.org).

Y. Wang is with the College of Electrical and Information Engineering, Hunan University, Changsha, 410082 China (e-mail: yaonan@hnu.edu.cn).

G. Liu is with the School of Computer and Communication, Hunan Institute of Engineering, Xiangtan 411104 China (email: lgr@hnie.edu.cn).

ELECTRIC vehicles (EVs) will play a vital role in future's transportation systems since this technology is promising for both energy security and environment. One vital issue is that whether nowadays' power grid can sustain the growing demand due to the growing number of EVs and by what method to charge these vehicles. To address these concern, in recent years, many researchers have studied the 'V2G' technology[1]-[3], which means EVs serve in both charge and discharge mode and realize bi-directional power flow between cars and power lines. Former studies[1]-[15] have shown that, V2G system is able to provide additional opportunities for grid operators, such as reactive power support[6], active power regulation, load balancing by valley filling and peak load shaving[7][8], and is able to provide ancillary services such as frequency control and spinning reserves[9]-[12] so that the grid efficiency[13]-[15] is improved. These studies, however, are mainly focused on the power system scheduling with aggregated EVs, which largely depends on the communication between the Independent System Operator (ISO) and the EV aggregators, and lack necessary study for low-level control.

Usually, EVs are connected to the power grid through power electronic converters. So does all kinds of renewable energy sources. In general, when the penetration of EVs and renewable sources are relatively low, the stability of the power grid can be held by the large synchronous generator which is widely used in conventional thermal power plants or hydro power plants. However, as the trend of EVs and renewable sources' penetration is going high in futures' power grid, the large synchronous generator is likely no longer able to hold the stability of the whole power grid. The key problem is, the power electronic converter, which is widely used as the interface for EVs and renewables to plug in the power grid, lacks damping and inertia and does not have the same synchronous characteristic as the synchronous generator does. Hence, when the penetration of EVs and renewables is high, the power grid might lose its' robustness when power fluctuation and failure occurs. To address the problem, Researchers have proposed a so-called 'virtual synchronous machine (VSM)' [16][17] method to control the power electronic converter so that it can mimic the dynamic characteristic of a real synchronous machine. Synchronverter[18] is a kind of VSM. It's' controller has embedded the same mathematical model of a real synchronous machine so that a grid-connected synchronverter can behave like a real grid-connected synchronous machine and is able to realize autonomous frequency and voltage regulation for the grid due to its' inner frequency- and voltage- drooping mechanism. Additionally, it is worth mention that synchronverter technology is a voltage-controlled strategy, converters equipped by which are able to provide voltage support to the grid when the grid is weak while conventional current-controlled strategies(for eg., PQ control strategy) are not able to[19].

In this paper, an original control method is proposed to control the bi-directional converters of a V2G supporting charging station(CS) based on the synchronverter technology[18][19]. The CS is composed of several CS units connected in parallel and using synchronverters as the AC/DC interfaces between each CS units and the grid. A T-S fuzzy controller is designed to decide the reference set power of the synchronverter, which also translates the real power-frequency (P-f) control characteristic control characteristic of the synchronverter, by considering the grid frequency (which is estimated by the synchronverter itself) and the battery status of each individual EV inside the unit; An adaptive frequency drooping coefficient mechanism is designed to modify the imaginary mechanical friction coefficient to adapt the change of the energy capacity of the DC bus. A power distribution strategy is proposed to distribute the total real power of a CS unit to every EVs inside it and ensure the charging/discharging power of each EV is subject to its' maximum limit. By using the proposed method, a CS can be integrated into the power grid and behave in the same way as large synchronous machine do, so that the CS equipped with the proposed control strategy and the power grid can be held as a whole, hence the power system itself is more robust to disturbance such as frequency fluctuation or failure. It has already been demonstrated by over 100 years operation in the power system that the synchronization mechanism of synchronous machines is able to hold the stability of the power system. Additionally, a synchronverter based V2G charging station adds damping and inertia to the power grid, which would help the operation of the grid be more smoother[19]. This characteristic is vital when the penetration level of EVs is large. The proposed CS is able to not only realizing smart bi-directional charging control of electric vehicles regarding EVs' SoC and grid status but also providing high-quality frequency and voltage regulation services for the grid due to the inner frequency- and voltage-drooping mechanisms of the synchronverter.

The rest of this paper is organized as follows. Section 2 introduced the structure and the basic idea of operating the proposed V2G charging station(CS). The synchronverter technology is overviewed in Section 3. Section 4 proposed a synchronverter-based control strategy for the proposed V2G charging station, where a T-S fuzzy controller is designed to generate the reference set power of the synchronverter, and an adaptive drooping coefficient mechanism is proposed to ensure the safety of the frequency droop operation. Additionally, a power distribution strategy is proposed for control of power flow between different EVs. The performance of the proposed strategy is tested by simulations in the different scenario and the results are discussed in Section 5. Finally, conclusions are given in section 6.

II. Modeling of a V2G Charging Station for Electric Vehicles

The proposed V2G charging station (CS) for electric vehicles is composed of several CS units connected in parallel, where a CS unit is consist of three subunits: Control Unit (CU), Synchronverter (SV), and DC Unit. SV is functioned as a bi-directional converter that combines the grid and the DC unit, its' reference set power and imaginary mechanical friction coefficient is determined by the control unit, which is composed of four parts: capacity calculation unit, T-S fuzzy control unit, and power distribution unit, and adaptive drooping coefficient unit; DC unit is composed of a DC bus, several EVs that connected to the DC bus, and DC-DC converters. The layout of a CS unit is as Fig.1 shown. The operation process of a proposed CS unit is summarized as follows:

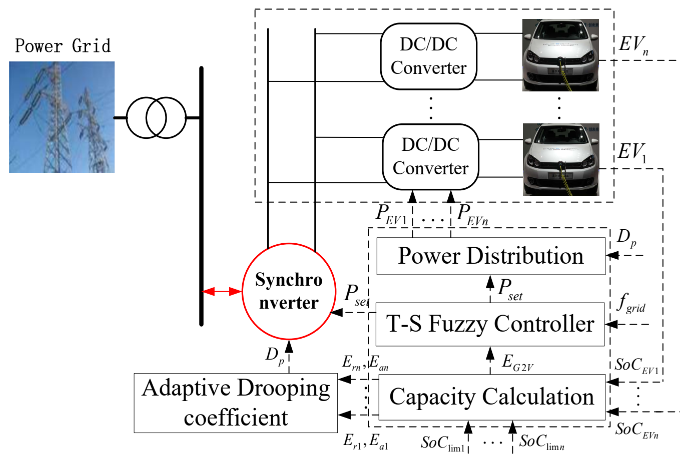

Fig. 1. Conceptual system framework

1) All the information of EVs' state of charge $(SoC_1, SoC_2, \cdot\cdot\cdot, SoC_n)$ and constraints $(SoC\min_1, SoC\min_2, \cdot\cdot\cdot, SoC\min_n)$(where $SoC\min_i$ are the lower SOC limit of EV batteries defined by EV users) are collected and send to the capacity calculation unit of the CCU;

2) The capacity calculation unit of the CCU count out the individual available energy $(E_{a1}, E_{a2}, \cdot\cdot\cdot, E_{an})$ as well as the individual required energy $(E_{r1}, E_{r2}, \cdot\cdot\cdot, E_{rn})$ of each EVs' batteries and then calculate out the total available energy (E_{V2G}) and the total required energy (E_{G2V}) of the CS unit;

3) Based on the grid frequency (f_{grid}) (which is estimated by the synchronverter itself) and the total required energy (E_{G2V}), the T-S fuzzy controller calculate out the reference set power (P_{set}) of the CS unit;

4) According to the total available energy (E_{V2G}), select a proper frequency drooping coefficient of the synchronverter;

5) According to the result of T-S fuzzy controller P_{set} and the selected frequency drooping coefficient of the synchronverter, according to the individual available energy $(E_{ai}$, the individual required energy $(E_{ri}$, as well as the maximum power limit of each EVs, calculate out the reference charging/discharging power $(P_{EV1}, P_{EV2}, \cdot\cdot\cdot, P_{EVn})$ of each EVs and the final set power $P_{set}^{'}$ of the synchonverter simultaneously;

6) According to the calculation results in step 4 and step5, set and run the synchronverter to realize the autonomous interaction between the CS and the grid.

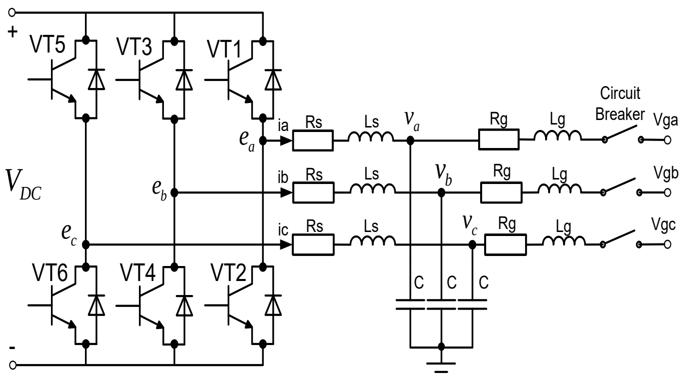

Fig. 2. Power Part of a Synchronverter

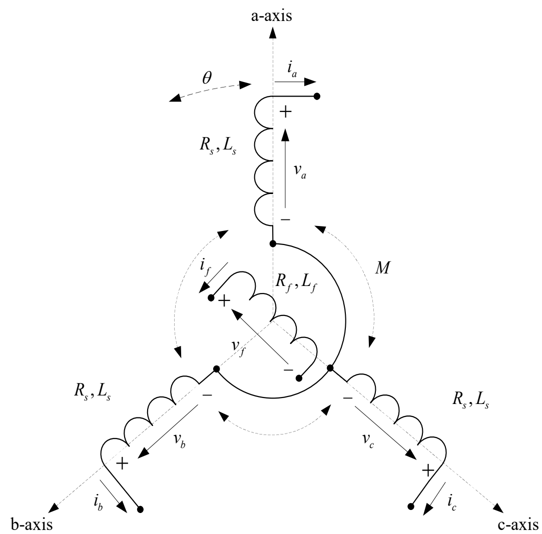

Fig. 3. Structure of an idealized three-phase round-rotor synchronous machine

III. Overview of the Synchronverter Technology

In this paper, synchronverters, which are converters that mimic synchronous machines[18][19], is introduced and operated here as the bi-directional DC-AC converter between the DC bus and the grid. The power part of a synchronverter is as Fig.2 shown. Imaging that the inductance L_s and resistance R_s of the LC filter are the impedance of stator windings of an imaginary synchronous generator(SG) as Fig.3 shown, the capacitor voltage $[v_a, v_b, v_c]^T$ is the terminal voltage of the SG, the inductor current $[i_a, i_b, i_c]^T$ is the stator current of the imaginary SG. The mathematical model of an SV can be formulated as figure 4 shown, which includes the mathematical model of a three-phase round-rotor synchronous machine described by:

$$\ddot{\theta} = \frac{1}{J}\left(T_m - T_e - D_p\dot{\theta}\right) \tag{1}$$

$$T_e = M_f i_f \left\langle i, \widetilde{sin}\theta \right\rangle \tag{2}$$

$$e = \dot{\theta} M_f i_f \widetilde{sin}\theta \tag{3}$$

$$Q = -\dot{\theta} M_f i_f \left\langle i, \widetilde{cos}\theta \right\rangle \tag{4}$$

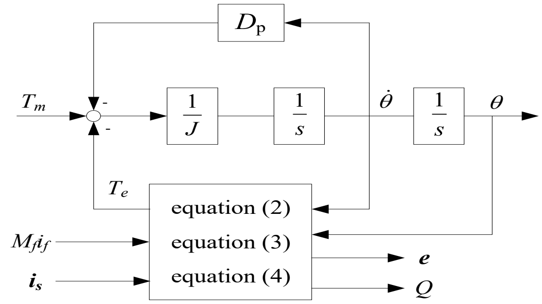

Fig. 4. Mathematical model of a synchronverter

In Fig.4, T_m is the mechanical torque of the rotor, which is also the control input of the SV; T_e is the electromagnetic torque of the rotor; J is the imaginary moment of inertia of rotor; D_p is the imaginary mechanical friction coefficient of rotor (which is also the drooping coefficient of frequency droop control loop); i_f is the field excitation current and M_f is the mutual inductance between the stator windings and the field winding; θ is the rotor angle while $\dot{\theta}$ is the virtual angular speed of the machine; i is the stator current flowing out of the machine; Q is the reactive power; e is the back EMF due to the movement of the imaginary rotor; $\widetilde{sin}\theta$ and $\widetilde{cos}\theta$ are defined as:

$$\widetilde{\sin}\theta = \begin{bmatrix} \sin\theta \\ \sin\left(\theta - \frac{2\pi}{3}\right) \\ \sin\left(\theta + \frac{2\pi}{3}\right) \end{bmatrix}, \widetilde{cos}\theta = \begin{bmatrix} \cos\theta \\ \cos\left(\theta - \frac{2\pi}{3}\right) \\ \cos\left(\theta + \frac{2\pi}{3}\right) \end{bmatrix} \tag{5}$$

After mathematical modeling of the SV, the model will be embedded in the DSP controller of a three phase converter, the back EMF e is the control signal sent to the PWM generator. According to the 'area equivalence principle', it can be concluded that refer to Fig.2, after filtering the output voltage e of the converter through the LC filter, the voltage on the capacitor C can be equivalent to the virtual stator voltage. It can be seen that if the mathematical model and the real synchronous generator are given with the same input – the prime mover mechanical torque, magnetic inductance and excitation current of a synchronous machine, the same output voltage as the stator side of the real synchronous generator can be obtained on the bridge arm of the SV. Since the internal mathematical principles, as well as the external physical representation, are the same as a real synchronous machine, the synchonverter is also called virtual synchronous machine.

IV. Synchronverter-based Control Strategy for the Proposed V2G Charging Station

In this section, a synchronverter-based control strategy for the V2G charging station is proposed as Fig.5 shown. The upper part of Fig.5 is the frequency droop control loop which is designed for regulating real power, or to say, charging and discharging power of the charging station; the lower part of Fig.5 is the voltage droop control loop, by which the charging station is able to provide the grid reactive power for voltage support.

In frequency droop control loop, $\dot{\theta}_n$ is the nominal frequency of the grid, $\dot{\theta}_r$ is the reference frequency of real power droop

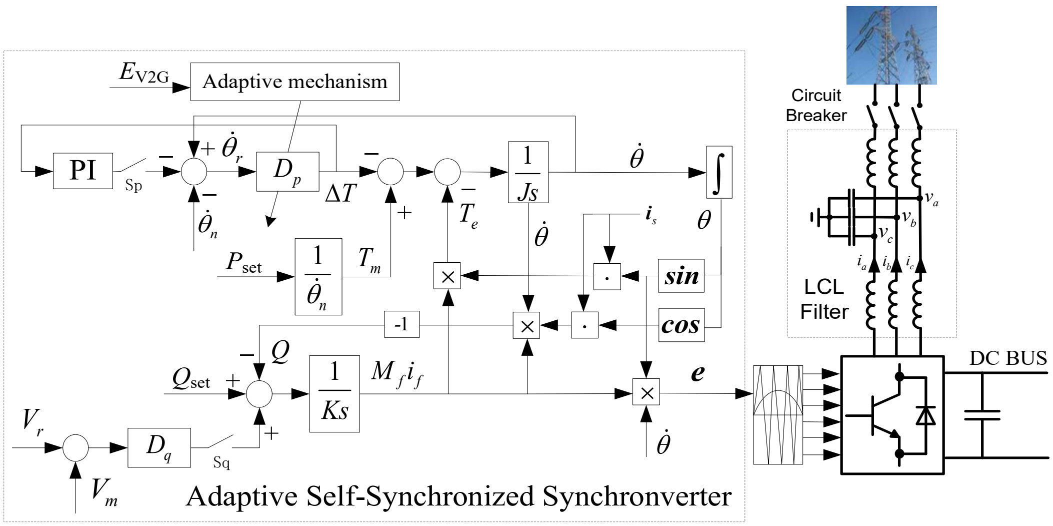

Fig. 5. Control of a Synchronverter(SV)

control, a PI controller is adopted to regulate the output ΔT of the frequency droop block to be 0 and to generate a small $\Delta\dot{\theta}_r$, $\Delta\dot{\theta}_r$ is then added to the nominal frequency $\dot{\theta}_r$ so that $\dot{\theta}_r$ is generated which is nearly the same as the grid frequency. Detail demonstration of this self-frequency tracking performance can be found in the literature[20]. Based on this self-frequency tracking performance, an SV do not need a dedicated synchronization unit, for e.g., a phase-locked loop(PLL), to provide phase references. This have simplify the operation of controller, reduced cost and free of control error caused by the use of PLL.D_p is the drooping coefficient of frequency droop control, which is defined as:

$$D_p = -\frac{\Delta T}{\Delta\dot{\theta}} \approx \frac{\Delta P}{\Delta\dot{\theta}\cdot\dot{\theta}_n} = \frac{P_n \cdot x\%}{\left(\dot{\theta}_n\right)^2 \cdot y\%} \tag{6}$$

Where P_n is the rated real power of synchronverter, $\dot{\theta}_n$ is the nominal grid frequency, the physical meaning of equation (6) is: a drop of x% of grid frequency cause the torque(also the real power) increase by x%.

J is the virtual inertia of rotor, which is defined by D_p and the time constant of frequency loop τ_f:

$$J = D_p\tau_f \tag{7}$$

In voltage droop control loop, V_n is the nominal value of grid voltage amplitude, V_m is the amplitude of grid voltage, which is calculated by (assuming the terminal voltage are balanced):

$$V_aV_b + V_bV_c + V_cV_a = -\frac{3}{4}V_m^2 \tag{8}$$

D_q is defined as the ratio of the required change of reactive power ΔQ to the change of voltage Δv:

$$D_q = -\frac{\Delta Q}{\Delta V} = \frac{Q_n \cdot x\%}{V_n \cdot y\%} \tag{9}$$

Where Q_n is the rated reactive power of synchronverter, the physical meaning of equation (9) is: a drop of y% of grid voltage causes the reactive power increase by x%.

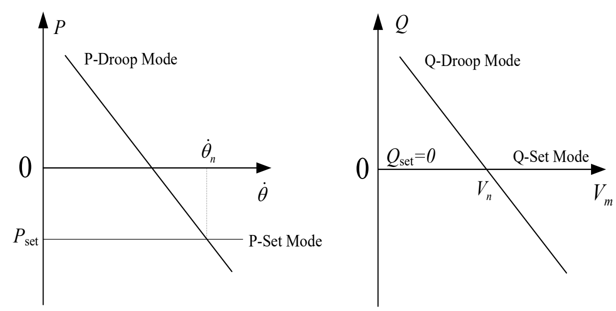

Fig. 6. P-f and Q-V control characteristic of the synchronverter

The error between the reference value Q_{ref} and the reactive power Q is fed into an integrator with a gain 1/K to generate M_fi_f, where K is defined by D_q, nominal grid frequency $\dot{\theta}_n$ and the time constant of voltage loop τ_v:

$$K = \dot{\theta}_nD_q\tau_v \tag{10}$$

The real power-frequency (P-f) control characteristic and reactive power-voltage (Q-V) control characteristic of the synchronverter is as Fig.6 shown.

It can be seen from Fig.6, when SV work in P-set mode, the output power of SV track the reference P_{set}, which means the power output of the virtual prime mover; when synchronverter work in P-droop mode, the output power of SV is a linear function of the grid frequency. The slash shown in fig.6 will be translated according to the position of the reference P_{set}. D_p is the slope of the slash. Obviously, a greater D_p means the same frequency change would cause larger real power change in response. Q-set mode and Q-droop mode are similar to P-set mode and P-droop mode, no more tautology here.

Different operation modes of the SV can be selected by turn on or off switches shown in table 2. In this paper, when the grid frequency is higher than its nominal value, the synchronverter is operated in P-set, Q-droop mode; When the grid frequency is equal to or lower than its nominal value, and the total available

TABLE I
OPERATION MODES OF A SYNCHRONVERTER

Switch Sp	Switch Sq	Mode
ON	ON	P-Set, Q-Droop
ON	OFF	P-Set, Q-Set
OFF	ON	P-Droop, Q-Droop
OFF	OFF	P-Droop, Q-set

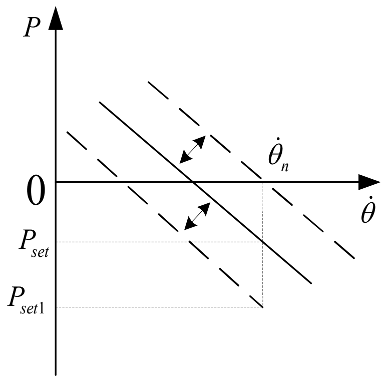

Fig. 7. Different P_{set} translate the P-f control characteristicr of the SV

energy of the CS unit $E_{V2G} > 0$, the SV is operated in P-droop, Q-droop mode.

A. Decision of P_{set}

As been discussed above, the P-f control characteristic of the SV can be translated by given different reference set power P_{set} as Fig.7 shown. The basic idea of translating the P-f control characteristic is the concept of secondary frequency control in power system. The virtual prime mover will raise up its' real power output when the grid frequency is dropping and will cut down it when the grid frequency is raising. Considering the particularity of the EV charging station, the reference set power P_{set} should also refer to the battery status of EVs inside the charging station. Hence, a T-S fuzzy controller is adopted here to decide the reference set power, which is also the quantity of the translation of the P-f control characteristic of the SV.

1) capacity calculation: According to EVs' state of charges and constraints, the individual available energy E_{ai} , the individual required energy E_{ri}, as well as the maximum capacity of each EVs' batteries E_{maxi} can be calculated by:

$$E_{ai} = \begin{cases} V_{ti}Q_i\left(SoC_i - SoC\min_i\right) & E_{ai} \geq 0 \\ 0 & E_{ai} < 0 \end{cases} \tag{11}$$

$$E_{ri} = \begin{cases} V_{ti}Q_i\left(100\% - SoC_i\right) & E_{ri} \geq 0 \\ 0 & E_{ri} < 0 \end{cases} \tag{12}$$

$$E_{maxi} = V_{ti}Q_i \tag{13}$$

where V_{ti} and Q_i are the terminal voltage and the rated capacity of the EVi's battery respectively[22].

Then the total available energy (E_{V2G}) and total required energy (E_{G2V}) of the CS unit can be calculated by:

$$\begin{cases} E_{V2G} = \sum\limits_{i=1}^{n} E_{ai} \\ E_{G2V} = \sum\limits_{i=1}^{n} E_{ri} \end{cases} \tag{14}$$

2) T-S fuzzy control: As mentioned above, a T-S fuzzy controller is designed to generate the reference charging power P_{ref} for the CS unit according to the value of f_{grid} and E_{G2V}. The triangular membership function is used here to define fuzzy variables ($\tilde{f}_{grid}$ and $\tilde{E}_{G2V}$) as it is easier to calculate:

$$\mu_{\tilde{A}}(x) = \begin{cases} (x-l)/(m-l) & l < x \leq m \\ (r-x)/(r-m) & m < x \leq r \\ 0 & \text{otherwise} \end{cases} \tag{15}$$

where l and r are the lower and upper limits of the fuzzy number $\tilde{A}$ and m is the middle value.

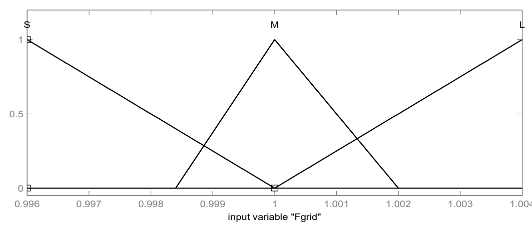

(a) Membership function for $\tilde{f}_{grid}$

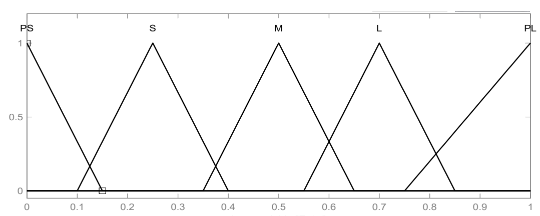

(b) Membership function for $\tilde{E}_{G2V}$

Fig. 8. Membership function of the two fuzzy sets

The discourse domain of fuzzy variable $\tilde{f}_{grid}$ is [0.996, 1.004], which is transferred from f_{grid}'s original domain [49.8, 50.2]. Three fuzzy subsets (Small(S), Middle(M), Large(L)) have been chosen for $\tilde{f}_{grid}$ as Fig.8(a) shown.

The discourse domain of fuzzy variable $\tilde{E}_{G2V}$ is [0,1], which is transferred from E_{G2V}'s original domain [0, E_{max}], where E_{max} is a variable that related to the number of EVs integrated in a CS unit:

$$E_{max} = \sum_{i=1}^{n} E_{maxi} \tag{16}$$

Five fuzzy subsets (Plus Small(PS), Small(S), Middle(M), Large(L), Plus Large(PL)) have been chosen for $\tilde{E}_{G2V}$ as Fig.8(b) shown.

The rule of FLC is as (17) shown:

$$\begin{array}{l} R_a^i : if \quad x_1 \quad is \quad A_1^i \quad and \quad x_2 \quad is \quad A_2^i \\ then \quad p_c^i = f^i(x_2) \\ i = 1, 2, \cdots, m \end{array} \tag{17}$$

TABLE II
RULE BASE FOR FLC

$\tilde{f}_{grid}$	$\tilde{E}_{G2V}$	λ_a^i	λ_b^i	$\tilde{f}_{grid}$	$\tilde{E}_{G2V}$	λ_a^i	λ_b^i
S	PS	1	0	M	L	0	0.8
S	S	0	0.3	M	PL	0	1
S	M	0	0.5	L	VS	1	0
S	L	0	0.5	L	S	0	0.5
S	PL	0	0.8	L	M	0	0.5
M	PS	1	0	L	L	0	0.8
M	S	0	0.3	L	PL	0	1
M	M	0	0.5				

where $x_1 = f_{grid}$, $x_2 = E_{G2V}$, $A_1^i \in \tilde{f}_{grid}$, $A_2^i \in \tilde{E}_{G2V}$. p_c^i is the charging power of the CS unit determined by rule i, which is designed here as a linear function of E_{G2V}:

$$p_c^i = f^i(x_2) = \frac{\lambda_a^i}{T_0} E_{G2V} + \lambda_b^i n P_{cm} \tag{18}$$

where n is the number of EVs in the CS unit, P_{cm} is the nominal charging power of electric vehicles, T_0 is a time constant, which can be calculated by:

$$T_0 = \frac{MAX(E_{maxi})}{P_{cn}} \tag{19}$$

$\lambda_a^i \in [0,1]$ and $\lambda_b^i \in [0, 0.3, 0.5, 0.8, 1]$ are constants which value are determined by the value of E_{G2V} and f_{grid}. If the required energy E_{G2V} is very small, then λ_a^i equals to 1 and λ_b^i equals to 0 so that p_c^i is able to track the change of E_{G2V}, hence the battery of EVs won't be overcharged; If E_{G2V} is not very small, λ_a^i equals to 0 and λ_b^i equals to 1 so that the value of p_c^i is self-adjusted according to E_{G2V} and f_{grid}. The rule base for selection of λ_a^i and λ_b^i is given in Table 1.

According to table 1, the output of FLC is formulated as:

$$P_{set} = \frac{\sum_{i=1}^{15} p_c^i \prod_{l=n}^{2} \mu_{A_n^i}(x_n)}{\sum_{i=1}^{15} \prod_{n=1}^{2} \mu_{A_n^i}(x_n)} = \bar{f}_1(x_1,x_2) E_{G2V} + \bar{f}_2(x_1,x_2) \tag{20}$$

where $\bar{f}_1(x_1,x_2)$ and $\bar{f}_2(x_1,x_2)$ are non-linear functions:

$$\begin{cases} \bar{f}_1(x_1,x_2) = \dfrac{\sum_{i=1}^{15} \lambda_a^i \prod_{n=1}^{2} \mu_{A_n^i}(x_n)}{\sum_{i=1}^{15} \prod_{n=1}^{2} \mu_{A_n^i}(x_n)} \cdot \dfrac{1}{T_0} \\ \bar{f}_2(x_1,x_2) = \dfrac{\sum_{i=1}^{15} \lambda_b^i \prod_{n=1}^{2} \mu_{A_n^i}(x_n)}{\sum_{i=1}^{15} \prod_{n=1}^{2} \mu_{A_n^i}(x_n)} \cdot nP_{cm} \end{cases} \tag{21}$$

After obtaining the current grid frequency and EV battery status at each sampling time, the reference charging power of each CS units can be calculated out by equation(20) and (21).

B. Adaptive frequency drooping coefficient

In this paper, The DC bus of the CS unit connects a number of EVs. Since the number and battery level of these EVs vary widely, it is hard to set a suitable frequency drooping coefficient for an SV in all possible energy storage situation of the DC bus when the SV is operated in P-droop mode. For e.g., if the total battery energy level of EVs connected to the DC bus is low(the number of EVs in the CS is small, or the SoC of EVs in the CS is low), a large frequency drooping coefficient may cause over discharge of EV batteries when the grid frequency is much lower than its' nominal value. if the total battery energy level of EVs connected to the DC bus is high, a relatively small frequency drooping coefficient can not achieve the best performance on frequency regulation. Hence, when the SV is operated in P-droop mode, it would be better if the frequency drooping coefficient can be self-adjusted according to the battery level of EVs connected to the DC bus.

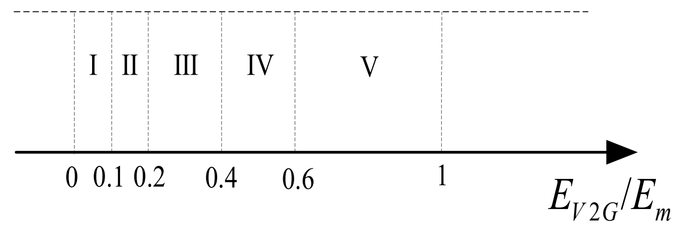

Fig. 9. battery level of a CS unit

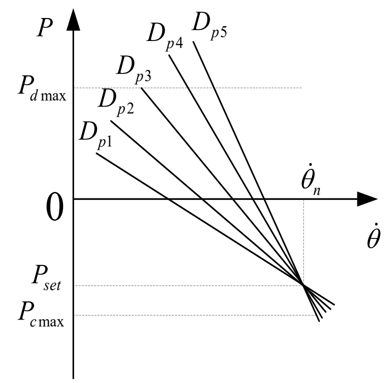

Fig. 10. P-f characteristic of the adaptive drooping coefficient synchronverter

According to the battery SoC limits set by EVs users, the total available energy E_{V2G} of a CS unit can be calculated out by equation (4). Assuming E_m is the maximum capacity of a CS unit, then the ratio of E_{V2G} to E_m can be divided into 5 parts within the closed interval [0,1] as fig.9 shown. If E_{V2G} / E_m is within the range V, which means the available energy for V2G of EVs is very high (and far from SoC lower limits), a large frequency drooping coefficient can be selected to achieve better frequency regulation performance. If E_{V2G} / E_m is within the range I, which means the number of EVs connected to the CS unit or the total available energy of the EVs is low, a small frequency droop coefficient should be selected to avoid over discharge. Based on the analysis above, assuming the rated power of the SV is 50kW, then the frequency droop coefficient of the SV can be chosen from Table 3, which is calculated by equation(6) and means a drop of 2.5%, 1.5%, 1%, 0.8%, 0.5% of grid frequency(from its' nominal value) respectively, causes the real power to increase by 100% . The P-f characteristic of the adaptive drooping coefficient SV is as fig.10 shown.

TABLE III
FREQUENCY DROOPING COEFFICIENT

Zone	I	II	III	IV	V
D_p	20.26	33.77	50.66	63.33	101.3

C. Power Distribution

A power distribution strategy is designed to distribute the input/output power of the SV to each EVs that connected to the DC bus of the CS unit. The charging/discharging power of the EVs can be calculated by equation(22).

$$\begin{cases} P_{EVi} = \frac{E_{ri}}{E_{G2V}} P_{G2V} + \frac{E_{ai}}{E_{V2G}} \left[D_p \dot{\theta}_n \left(\dot{\theta} - \dot{\theta}_n \right) \right] & \dot{\theta}_g \leq \theta_n \\ P_{EVi} = \frac{E_{ri}}{E_{G2V}} P_{G2V} & \dot{\theta}_g > \theta_n \end{cases} \tag{22}$$

where P_{EVi} is the reference power of each electric vehicles in the charging station. E_{V2G} and E_{G2V} are the total available and required energy of the CS unit, E_{ai} and E_{ri} are the available and required energy of each EV. By using the proposed strategy, the charging and discharging power of EVs are determined by the output of the fuzzy controller, grid frequency, the frequency drooping coefficient, individual EV required or available energy as well as the proportion that the required or available energy of each individual EV to the whole CS unit.

For safety concern, in order to prevent P_{EVi} exceed the maximum charging power P_{cm}, or the maximum discharging power P_{dm}, P_{EVi} is subject to constraint as equation (23) shown:

$$\begin{cases} P_{EVi} = P_{cm} & P_{EVi} \geq P_{cm} \\ P_{EVi} = -P_{dm} & P_{EVi} < -P_{dm} \end{cases} \tag{23}$$

Finally, the real power setpoint of the synchronverter $P_{set}^{'}$ turned out to be:

$$P_{set}^{'} = \begin{cases} -\sum_{i=1}^{n} P_{EVi} + D_p \dot{\theta}_n \left(\dot{\theta} - \dot{\theta}_n \right) & \dot{\theta} \leq \theta_n \\ -\sum_{i=1}^{n} P_{EVi} & \dot{\theta} > \theta_n \end{cases} \tag{24}$$

D. DC-DC Converters

The DC bus of the CS is connected with a series of EVs, the topology of the DC-DC converter for EVs is as Fig.11 shown, which is a bi-directional half-bridge buck-boost converter. If there is only one EV connected to the DC bus, the controller of the DC-DC converter is as Fig.12 shown, where the outer loop is to control the DC bus voltage and the inner loop is to control the inductor current, the charging/discharging power of the EV flow automatically. If the number of EVs connected to the DC bus more than one, then the controller for the first EV enters the CS unit is as Fig.11 shown, and the controller for the rest EVs are as Fig.13 shown, where P_{EVi} is divided by EV battery voltage(V_t) to obtain the reference current(I_{ref}) and then a PI controller is applied to control the current flow in or out the batteries[22].

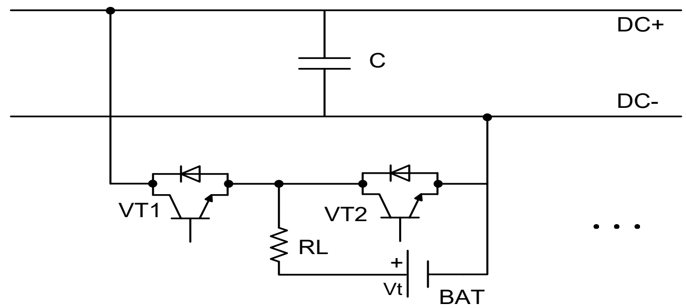

Fig. 11. Topology of DC-DC converter

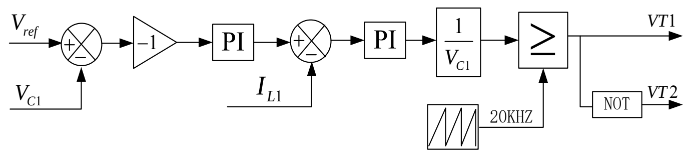

Fig. 12. DC-DC converter controller 1

V. Simulation Results and Discussion

Simulations were carried out in the environment of MATLAB R2015a/ SIMULINK/ Simscape/ SimPowerSystem. The solver used in the simulation was ode23tb with a relative tolerance of 10^{-3} and a maximum step size of 0.2ms. The parameters of the circuit used in the simulations are given in Table 4. The LCL filter design method is referred to the literature[23]. Three cases are considered for testing the effectiveness of the proposed CS with its' sychronverter based control strategy:

1) Case 1: EVs' batteries with different initial SOC connected during normal hours(assuming grid frequency is 1.0 p.u. at the beginning and will then drop to 0.999 p.u. at t=10s, grid voltage is 1.0 p.u.);

2) Case 2: EVs' batteries with different initial SOC connected during peak hours(assuming grid frequency is 0.996 p.u. at the beginning and will then raise up to 0.997 p.u. at t=10s, grid voltage is 0.98 p.u.);

3) Case 3: EVs' batteries with different initial SOC connected during valley hours(assuming grid frequency is 1.004 p.u. at the beginning and will then drop to 1.003 p.u. at t=10s, grid voltage is 1.02 p.u.).

Simulations were performed considering a V2G charging station include 3 CS units with 12 EVs in it (EV1-EV5 are with unit1, EV6-EV10 are with unit2, EV11-EV12 are with unit3). The different initial state of charge(SoC) and user defined SOC limits of each EV are given in Table 5. The rated capacity of each EV's battery is 100Ah, the rated battery voltage of

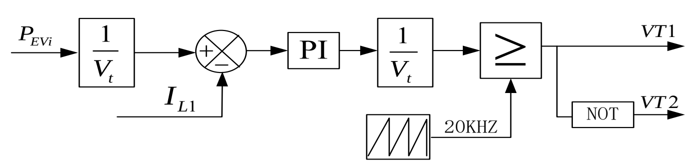

Fig. 13. DC-DC converter controller 2

TABLE IV
PARAMETERS OF THE SIMULATION CIRCUIT

Parameters	Values	Parameters	Values
L_s	150 μH	L_g	450 μH
R_s	0.045 Ω	R_g	0.135 Ω
C	22 μF	R	1000 Ω
L_{vr}	1 mH	R_{vr}	0.1 Ω
C_{dc}	10 mF	L_{dc}	20 mH
R_{dc}	0.1 Ω	K_p	0.02
K_i	0.4	DC-bus voltage	700 V
grid rated frequency	50 Hz	nominal voltage (line-line)	380 V

each EV is 300V. The power part of the charging station includes 3 parallel-operated SVs with 3 DC units connected to it. Assume the maximum charging and discharging power of each EV is P_{cm}=10kW, P_{dm}=-10kW; The rated real power of each synchronverter is 50kW, the rated reactive power of each SV is 10kVar; The voltage drooping factor D_q was chosen as 644.6(which means a voltage droop of 5% will cause the reactive power to increase by 100%). The time factor of the droop loops were chosen as $\tau_f = 0.002s$ and $\tau_v = 0.002s$.

TABLE V
BATTERIES SPECIFICATION IN DIFFERENT SCENARIO

i	SoC_{min}	Initial SoC		
		Case1	Case2	Case3
EV_1	10	50	50	50
EV_2	10	60	60	60
EV_3	10	70	70	70
EV_4	10	80	80	80
EV_5	10	95	95	95
EV_6	10	30	30	30
EV_7	10	40	40	40
EV_8	10	50	50	50
EV_9	10	80	80	80
EV_{10}	10	90	90	90
EV_{11}	10	60	60	60
EV_{12}	10	80	80	80

A. Case study

1) Case 1: EVs connected during normal hours: The period when the power grid is neither in peak hour or in valley hour here is called 'normal hour'. Assuming grid frequency is 1.0 p.u., grid voltage is 1.0 p.u., simulation results of SV internal frequency, real power, reactive power of the three CS units as well as battery current of EV1-EV12 are listed as Fig.14 shown. From Fig.14(a), it can be seen that the three SVs were quickly synchronized with the grid before the circuit breakers were turned on at t=0.5s. There was a tiny current surge on the circuit when grid connect operation was applied at t=0.5s. Then, at t=1 s, the SVs were quickly responded to the real power step change P_{set}(calculated by eq.19), since $\dot{\theta} = \dot{\theta}_n$, the value of P_{set} is mainly determined by the output of the T-S fuzzy controller according to the battery level of EVs in the charging station. It can be seen that, when EVs connected during normal hours, CS unit 1 to CS unit3 are all controlled to charge from the grid. As there are only 2 EVs in CS unit3, the charging power of unit3 is relatively lower than that of unit1 and unit2. Then, at t=10 s, the grid frequency drop to 0.999 p.u., it can be seen that the inner frequency of the SV track the grid frequency quickly, and the three CS unit response to the change of the grid frequency quickly by cutting down their charging power due to the frequency droop mechanism of the SV. As for the reactive power, as the grid voltage is the equal to its' nominal value, most of time the reactive power of the three SV is the same as Q_{set} which was always set as 0. but at t=0.5s, and t=1s, Q faced a little fluctuation due to the coupling between real and reactive power. From Fig.14(b), it can be seen that the battery current of EVs in each CS unit is changing according to the real power change of the CS unit. the EVs share the real power of the CS unit according to their own battery status: as the user soc limit are set the same, the EV with lower battery SoC will gain more charging power (hence the battery charging current is higher) according to the proposed power distribution strategy(such as EV1-EV3, EV6-EV8, EV11), while the battery charging current of EVs with high battery SoC is relatively low(such as EV4-EV5, EV9-EV10, EV12).

2) Case 2: EVs connected during peak hours: When EVs connected during peak hours, simulation results of SV internal frequency, real power, reactive power of the three CS units as well as battery current of EV1-EV12 are listed as Fig.15 shown. From Fig.15(a), it can be seen that the internal frequencies of the three SVs were quickly synchronized with the grid frequency. because the grid frequency is lower than its' nominal value, the three SV are operated in P-droop, Q-droop mode, the frequency drooping coefficient D_p will be adaptively selected according to the battery status of EVs connected to the DC buses of the SVs. It can be seen that, at t=1s, CS unit1 and CS unit3 are controlled to discharge energy to the grid, while unit2 is controlled to charge from the grid. The value of the charging/discharging power of the three CS unit are determined both by the T-S fuzzy controller and the frequency drooping mechanism of the SVs. As the battery level of CS unit1 is relatively high, then a relatively high D_p is applied. According to P-f characteristic of SV , when $\dot{\theta} - \dot{\theta}_n < 0$, the CS unit will reduce the charging power or discharge to the grid (depend on the value of P_set). In this case, since the battery level of CS unit1 is relatively high, then the basic charging power of CS unit1 determined by the T-S fuzzy controller is relatively low, so a 0.4% deviation of grid frequency lead CS unit1 discharge energy to the grid. The energy stored in CS unit2 is lower than unit1, so it still charging from the grid. However, when compared with case1, it can be seen that the charging power of CS unit2 is greatly reduced, which is also due to the P-f control characteristic of the SV. There are only 2 EVs in CS unit3, hence a relatively low D_p is applied. So the discharging power of CS unit3 is lower than that of unit1. Then, at t=10 s, the grid frequency raise up to 0.997 p.u.,the inner frequency of the SV track the grid frequency quickly, and the three CS

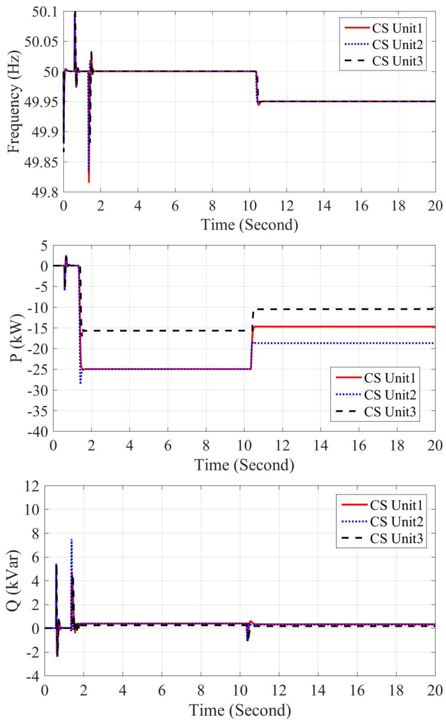

(a) SV internal frequency, real and reactive power of the CS unit 1-3

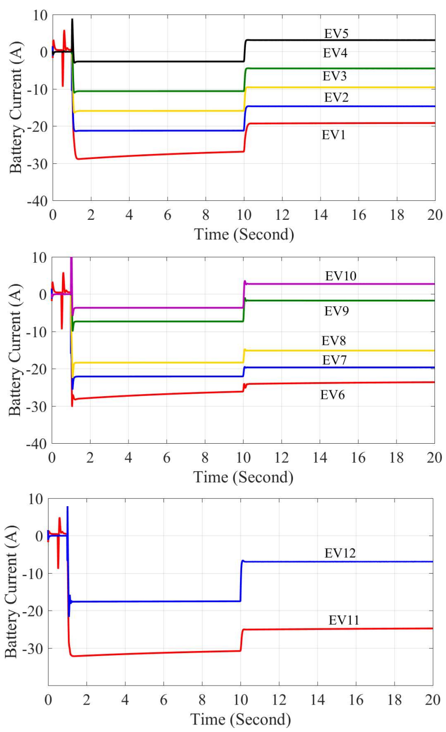

(b) Battery current of EV1-12

Fig. 14. Simulation results of case 1

unit response to the change of the grid frequency quickly by cutting down their discharging power or to say, raising up their charging power due to the frequency droop mechanism of the SVs. As for reactive power, as the grid voltage is 2% lower than its nominal value, the reactive power of each SV raised up about 4kVar at t=1s. From Fig.15(b), it can be seen that the battery current of EVs in each CS unit is changing according to the real power change of the CS unit. As the user soc limit are set the same, the EV with lower battery SoC has a positive battery charging current, which means they are charging energy from the DC bus (such as EV1, EV6-EV8), while the battery charging current of EVs with high battery SoC is discharging(such as EV2-EV5, EV9-EV10).

3) Case 3: EVs connected during valley hours: The valley hours of the grid mainly at midnight. When EVs connected during valley hours, simulation results of SV internal frequency, real power, reactive power of the three CS units as well as battery current of EV1-EV12 are listed as Fig.16 shown. Because the grid frequency is higher than its' nominal value, the three SVs of the CS units are operated in P-set, Q-droop mode. From Fig.16(a), it can be seen that, at t=1s, all three CS units are controlled to absorb energy from the grid with different charging power.The value of real power is determined by T-S fuzzy controllers according to the energy requirement of each EVs inside the unit. It can be seen that the battery level of CS unit1 is higher than unit2, hence the charging power of unit1 is lower than unit2. Unit3 only contain 2 EVs, hence its' charging power is the lowest among the three unit. At t=10 s, the grid frequency drops up to 1.003 p.u, since which is still higher than its' nominal value, the three SVs of the CS units are operated in P=set mode, to avoid overcharge, the real power of the three CS units keep the same value as P_set. As for reactive power, as the grid voltage is 2% higher than its nominal value, the reactive power of each SV dropped by about 4kVar at t=1s. From Fig.16(b), it can be seen that, as the user soc limit are set the same, the EV with lower battery SoC is charging with higher power (such as EV1-EV2, EV6-EV8, EV11), while the battery charging current of EVs with high battery SoC is charging with low power(such as EV4-EV5, EV9-EV10, EV12).

From the simulations above, it can be seen that although the initial SoC and user's limits of the EVs are the same among the three cases, the real power of the CS during peak hours, valley hours, and normal hours are quite different. The simulation results have shown the regulation ability of the CS to control the charging/discharging power of EVs in different grid scenarios.

Fig.17 have shown the changing of energy stored in the three CS units in case 1-3, where E_{g2v} is the total energy requirement of the CS unit and E_{v2g} is the total available energy of the CS unit. It can be seen in Fig.17 that in case 1 and case 3, while the grid frequency is the nominal value or higher than the nominal value, E_{g2v} of the three CS units is dropping and E_{v2g} is raising, which means the total energy level of the three CS units is increasing. In case 2, while the grid frequency is lower than the nominal value, E_{g2v} of CS unit1 and CS unit3 is raising and that of CS unit2 is dropping, the trend of E_{v2g} is just the opposite, which means the total energy level of CS unit1 and CS unit3 is decreasing, and that of CS unit2 is increasing. The change of energy stored in the three CS units in case 1-3 are consistent with the real power change of the three CS units shown in Fig.14 - Fig.16.

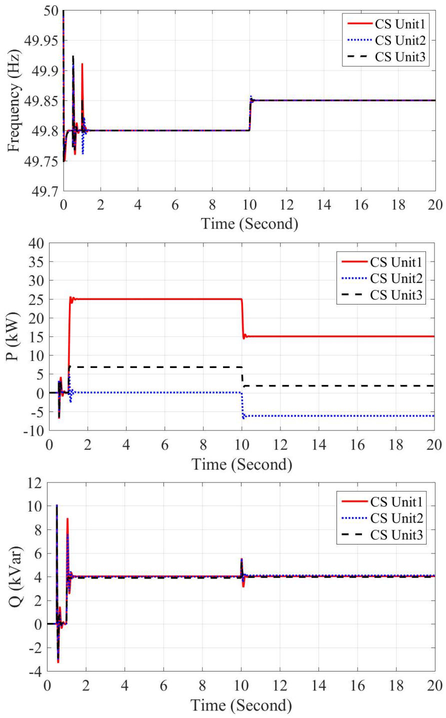

(a) SV internal frequency, real and reactive power of the CS unit 1-3

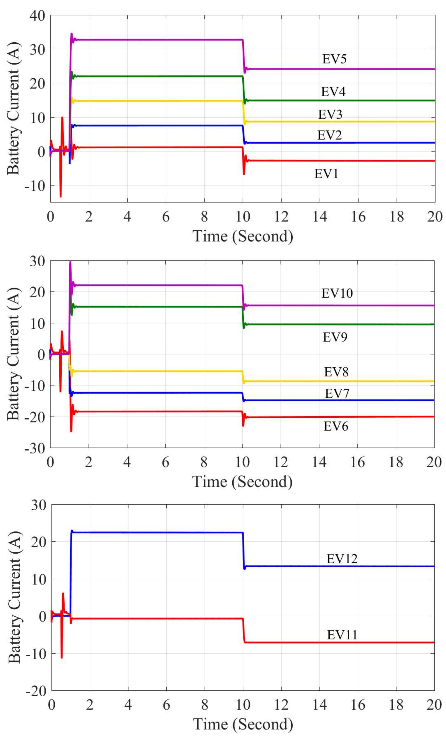

(b) Battery current of EV1-12

Fig. 15. Simulation results of case 2

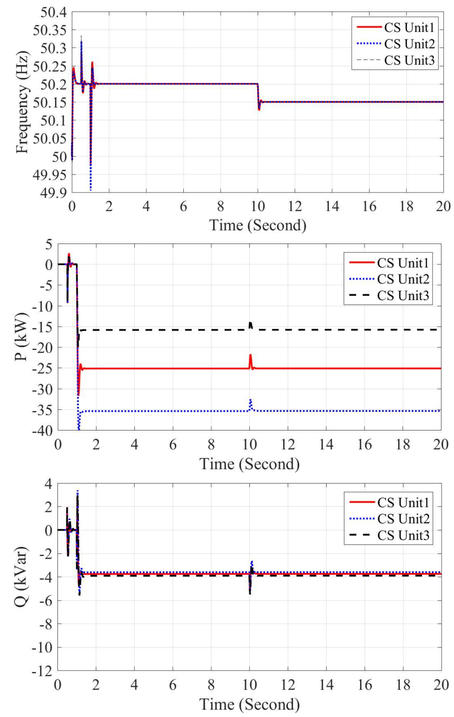

(a) SV internal frequency, real and reactive power of the CS unit 1-3

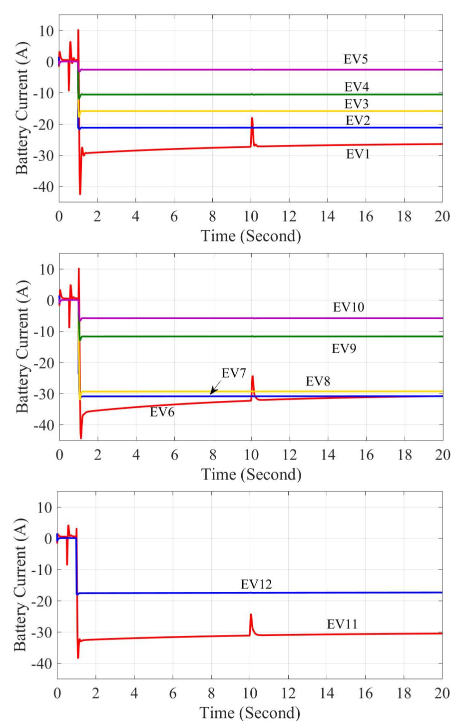

(b) Battery current of EV1-12

Fig. 16. Simulation results of case 3

B. Long-term simulation

A long-term simulation has been carried out by considering a proposed V2G charging station include 6 CS units with 30 EVs plugged into the grid at t=0h. Assuming that the 24-hour grid frequency is as Fig.18 shown. Assuming the SoC and the users' set of all the EVs in the charging station are the same as table 6 shown. The output power of the proposed V2G charging station in 24 hours are as Fig.19 shown, and the change of battery SoC in 25 hours is as Fig.20 shown:

From Fig.19 and Fig.20 it can be seen that, when the grid in valley hours(i.g. 0:00-6:00), the grid frequency is high,

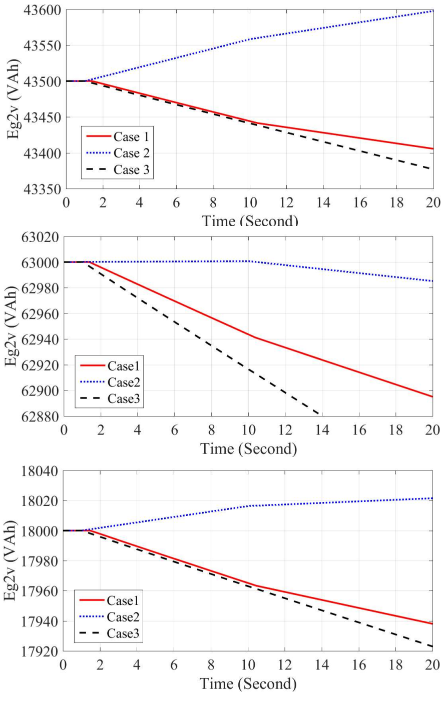

(a) Eg2v in three cases of the CS unit 1, unit2, unit3 respectively from top to bottom

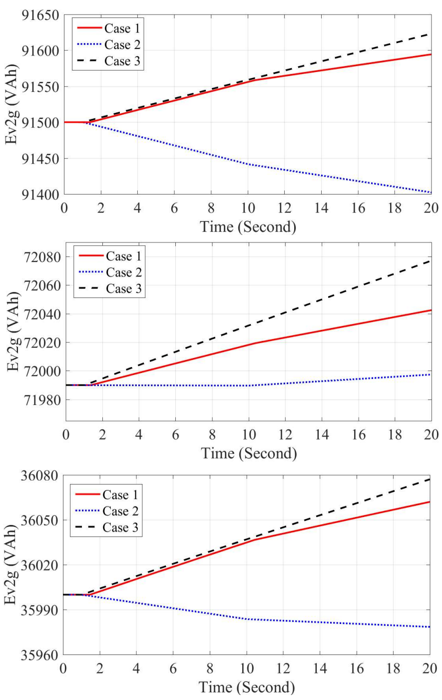

(b) Ev2g in three cases of the CS unit 1, unit2, unit3 respectively from top to bottom

Fig. 17. Energy stored of the three CS units in case 1-3

TABLE VI
BATTERY SPECIFICATION OF EVS FOR LONG-TERM SIMULATION

EV(i)	$Q_t i$	$V_t i$	SoC_{mini}	SoC_i
EV1-EV30	200Ah	300V	10%	10%

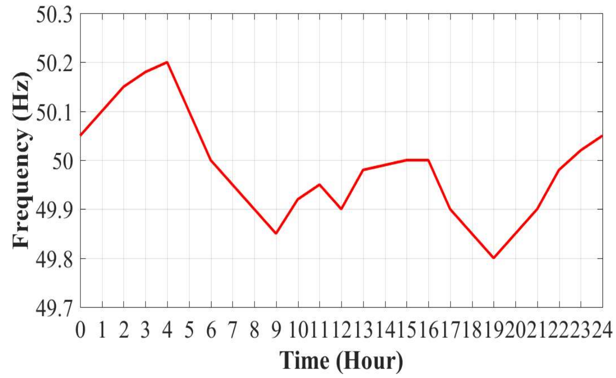

Fig. 18. 24 hour grid frequency

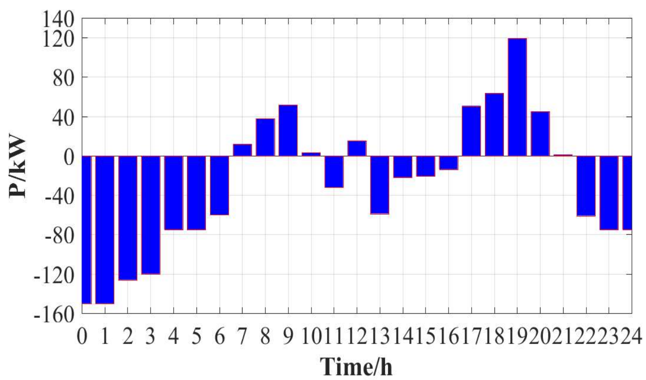

Fig. 19. 24 hour CS power output

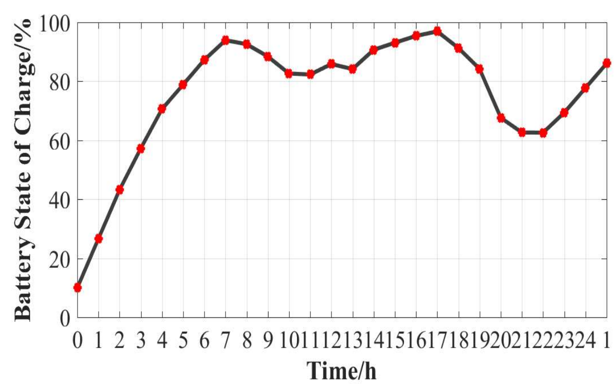

Fig. 20. 24 hour EV battery SoC curve

the CS is controlled to absorb excess energy from the grid, the battery SoC of EVs are raised up gradually. when the grid in peak hours(i.g. 7:00-21:00), the CS is controlled to feed energy back to the grid. It is worth mentioning that the value of charging or discharging power of the CS is not only related to the grid frequency but also related to the battery state of charge of EVs inside the CS. For eg., the grid frequency at 4 o'clock is higher than that of 3 o'clock, but the charging power of the CS at 4 o'clock is lower than that of 3'clock. This is due to the EVs' battery level at 4 o'clock is relatively high after 4-hour high power charge. As the energy require reduced, the charging power also reduced. It also can be seen that the grid frequency are the same at 9 o'clock and at 18 o'clock, which is lower than the nominal grid frequency. But the battery level of EVs at 18 o'clock is higher than that of 9 o'clock, thus the output power of the former is higher. At 19 o'clock, due to a sharp decrease in grid frequency, the discharging power of the CS jumped up rapidly, while at 20 o'clock, due to EVs have discharged a lot of energy to the grid, their battery SoC reduced so that their discharging power reduced as well. It can be seen from the long-term simulation that, the proposed V2G charging station is able to regulate its' input/output power according to the battery status of EVs inside the CS in different grid scenarios, it is able to provide frequency regulation service to the grid while meeting the energy demand of EV users.

Assuming the base load of the very grid that the CS is plugged in is the red line of fig.21 shown, according to fig.18, the load with the proposed V2G charging station can be calculated out as the blue line shown. Obviously, After employed the proposed V2G charging station, the peak load of the grid is cut down significantly, and the valley load is increased notably. The result of this simulation demonstrates that the proposed methodology is able to play a role of peak shaving and valley filling for the power network, thus promoting the efficiency of the electricity grid.

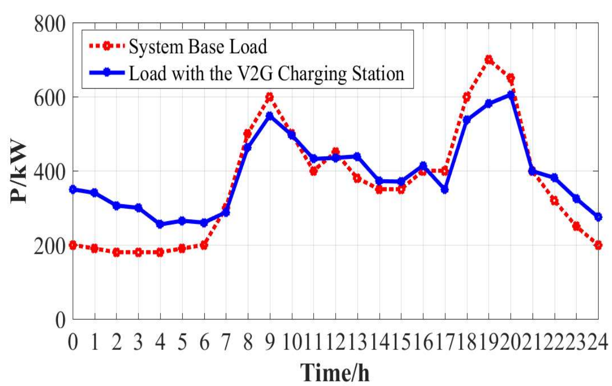

Fig. 21. 24 hour system load with and without the V2G charging station

VI. Conclusion

This work proposed a control method for V2G charging station based on the synchronverter technology. The CS is composed of several CS units connected in parallel and using synchronverters as the AC/DC interfaces between each CS units and the grid. The main features of the proposed method can be summarized as follows.

1) A T-S fuzzy controller is designed to decide the reference charging power of the CS unit according to the grid frequency(which is estimated by the synchronverter itself) and the charging demand of each individual EV inside the unit;

2) When synchronverter works in P-droop mode($\dot{\theta} \leq \theta_n$, $E_{V2G} > 0$), the output power of the CS unit is determined by the frequency droop control characteristic of the synchronveter, which means a drop of grid frequency would cause a decrease of reference charging power(or an increase of discharging power) of the CS unit in response.

3) An adaptive frequency drooping coefficient mechanism is designed to modify the frequency drooping coefficient(also the slope of the P-f control characteristic) of the synchronverter to adapt the change of the energy capacity of the DC bus;

4) By using the proposed method, a CS can be integrated into the power grid and behave in the same way as large synchronous machine do so that the CS equipped with the proposed control strategy and the power grid can be held as a whole based on the well-known synchronous mechanism. The proposed CS also adds damping and inertia to the power grid, which would help the operation of the grid be more smoother.

Simulation results have verified that the proposed strategy can not only effectively perform controlled charging/discharging of each single electric vehicle inside the CS, but providing high-quality frequency and voltage regulation services for the grid as well.

References

[1] Habib S, Kamran M, Rashid U. Impact analysis of vehicle-to-grid technology and charging strategies of electric vehicles on distribution networks - A review. *Journal of Power Sources*, **2015**, *277*, 205-214.

[2] Lund Peter D.; et al. Review of energy system flexibility measures to enable high levels of variable renewable electricity. *Renewable & Sustainable Energy Reviews*, **2015**, *45*, 785-807.

[3] Karfopoulos E.L.; K. A. Panourgias; and N. D. Hatziargyriou. Distributed Coordination of Electric Vehicles providing V2G Regulation Services. *IEEE Transactions on Power Systems*, **2016**, *31(4)*, 2834-2846.

[4] Yilmaz,M.; Krein,P. Review of impact of vehicle-to-grid technologies on distribution systems and utility interface. *IEEE Transactions on Power Electronics*, **2013**, *28(12)*, 5673-5689.

[5] K.F. Abdollah; T. Niknam; and M. Fotuhi-Firuzabad. Stochastic Reconfiguration and Optimal Coordination of V2G Plug-in Electric Vehicles Considering Correlated Wind Power Generation. *IEEE Transactions on Sustainable Energy* , **2015**, *6(3)*, 822-830.

[6] Kisacikoglu Mithat C.; B. Ozpineci; and L. M. Tolbert. EV/PHEV Bidirectional Charger Assessment for V2G Reactive Power Operation.*IEEE Transactions on Power Electronics*, **2013**,*28(12)*, 5717-5727.

[7] Zhang, Li, et al. Coordinating plug-in electric vehicle charging with electric grid: Valley filling and target load following.*Journal of Power Sources*, **2014**, *267(4)*, 584-597.

[8] Chen Niangjun; C. W. Tan; and T. Q. S. Quek. Electric Vehicle Charging in Smart Grid: Optimality and Valley-Filling Algorithms. *IEEE Journal of Selected Topics in Signal Processing*, **2014**, *8(6)*,1073-1083.

[9] Sarabi Siyamak; et al. Potential of vehicle-to-grid ancillary services considering the uncertainties in plug-in electric vehicle availability and service/localization limitations in distribution grids. *Applied Energy*, **2016**, *171*, 523-540.

[10] Sortomme,E.; El-Sharkwi,M.A. Optimal scheduling of vehicle-to-grid energy and ancillary services. *IEEE Transactions on Smart Grid*, **2012**,*3(1)*,351-359.

[11] Sekyung,H.; Soohee,H.; Sezaki,K. Development of an optimal vehicle-to-grid aggregator for frequency regulation.*IEEE Transactions on Smart Grid*, **2010**, *1(1)*,65-72.

[12] Liu Hui, et al. Decentralized Vehicle-to-Grid Control for Primary Frequency Regulation Considering Charging Demands. *IEEE Transactions on Power Systems*, **2013**, *28(3)*, 3480-3489.

[13] Noori Mehdi; et al. Light-duty electric vehicles to improve the integrity of the electricity grid through Vehicle-to-Grid technology: Analysis of regional net revenue and emissions savings. *Applied Energy*, **2016**, *168*, 146-158.

[14] Srivastava A.K.; Annabathina B.; Kamalasadan S. The challenges and policy options for integrating plug-in hybrid electric vehicle into the electric grid. *The Electricity Journal*, **2010**, *23(3)*, 83-91.

[15] Li,Z.; Guo, Q.; Sun,H.; et al. Emission-concerned wind-EV coordination on the transmission grid side with network constraints: Concept and case study. *IEEE Transactions on Smart Grid*, **2013**, *4(3)*, 1692-1704.

[16] Zhong, Qing Chang. "Virtual Synchronous Machines: A unified interface for grid integration." 3.4(2016):18-27. *IEEE Power Electronics Magazine*, **2016**, *3(4)*, 18-27.

[17] Zhong, Qing Chang. Power electronics-enabled autonomous power systems: next generation smart grids. *Wiley-IEEE Press*, **2017**

[18] Zhong QC, Weiss G. Synchronverters: Inverters that mimic synchronous generators. *Industrial Electronics, IEEE Transactions on.* ,**2011**, *58(4)*, 1259-67.

[19] Zhong QC, Nguyen PL, Ma Z, Sheng W. Self-synchronized synchronverters: inverters without a dedicated synchronization unit.*Power Electronics, IEEE Transactions on.* ,**2014**, *29(2)*, 617-30.

[20] Zhong, Qing Chang, and D. Boroyevich. Structural Resemblance Between Droop Controllers and Phase-Locked Loops. 4.99(2016):5733-5741. *IEEE Access*, **2016**, *4(99)*, 5733-5741.

[21] Takagi T, Sugeno M. Fuzzy identification of systems and its applications to modeling and control. *Systems, Man and Cybernetics, IEEE Transactions on.* , **1985**, *1*, 116-32.

[22] Thirugnanam Kannan; et al. Modeling and Control of Contactless Based Smart Charging Station in V2G Scenario. *IEEE Transactions on Smart Grid* , **2014**, *5(1)*, 337-348.

[23] Hatua Kamalesh; et al. Active Damping of Output LC Filter Resonance for Vector-Controlled VSI-Fed AC Motor Drives. *IEEE Transactions on Industrial Electronics*, **2012**, *59(1)*, 334-342.

[24] Emadi A, Ehasani M, Miller J M. Vehicular Electric Power Systems: Land, Sea, Air and Space Vehicle[M]. *New York Marcel Dekker*, **2003**.

[25] Ehsani A, Yimin Gao, Emadi A, Modern Electric, Hybrid Electric, and Fuel Cell Vehicles: Fundamentals, Theory, and Design[M]. *Boca Raton, FL, CRC Press*, **2005**.

Dongqi Liu received the B.S. degree in electronic information engineering from the University of Shanghai for Science and Technology, Shanghai, China, in 2008, and the Ph.D. degree in control science and engineering(awarded the Outstanding Graduates Prize) from Hunan University, Changsha, Changsha, China, in 2017. He has worked for Shanghai Electric Group Co. as an engineer from 2008 to 2010. He has worked in the Department of Electrical and Computer Engineering, Illinois Institute of Technology, Chicago as a visiting researcher from 2015 to 2016 under the sponsorship of Chinese Scholarship Council.

Since 2017, he has been a Lecturer in the School of Electrical and Information Engineering, Changsha University of Science&Technology. His research interests include electric vehicles, renewable energy, smart grid integration etc.

Qing-Chang Zhong received the Ph.D. degree in control and power engineering (awarded the Best Doctoral Thesis Prize)from Imperial College London, London, U.K., in 2004 and the Ph.D. degree in control theory and engineering from Shanghai Jiao Tong University, Shanghai, China, in 2000. He holds the Max McGraw Endowed Chair Professor in Energy and Power Engineering at the Dept. of Electrical and Computer Engineering, Illinois Institute of Technology, Chicago, USA, and the Research Professor in Control of Power Systems at the Department of Automatic Control and Systems Engineering, The University of Sheffield,UK. He is a Distinguished Lecturer of both the IEEE Power Electronics Society and the IEEE Control Systems Society. He proposed the architecture for the next-generation smart grids, which adopts the synchronization mechanism of synchronous machines to unify the interface and interaction of power system players with the grid and achieve autonomous operation of power systems. His research focuses on power electronics, advanced control theory and the integration of both, together with applications in renewable energy, smart grid integration, electric drives and electric vehicles, aircraft power systems, high-speed trains etc. He is a Fellow of IEEE, a Fellow of the Institution of Engineering and Technology (IET), the Vice-Chair of IFAC TC of Power and Energy Systems and was a Senior Research Fellow of the Royal Academy of Engineering/Leverhulme Trust, UK (2009-2010) and the UK Representative to the European Control Association (2013-2015).

Yaonan Wang received the B.S. degree in computer engineering from East China Technology Institute(ECTI), Fuzhou, China, in 1981, and the M.S. and Ph.D. degrees in control engineering from Hunan University, Changsha, China, in 1990 and 1994, respectively.

Since 1995, he has been a Professor with the College of Electrical and Information Engineering, Hunan University. His research interests include hybrid electric vehicle control, intelligent control theory and its applications.

Dr. Wang was a Senior Humboldt Fellow in Germany from 1998 to 2000 and from 2001 to 2004.

Guorong Liu received the B.S. degree and M.S. degrees in industrial automation from Hunan University, Changsha, China, in 1981 and 1986, respectively, and the Ph.D. degree in control engineering from Xi'an Jiaotong University, Xi'an, China, in 2003.

Since 1997, he has been a Professor with Hunan Institute of Engineering, Xiangtan, China. His research interests include intelligent control theory and applications and modern AC motor control.